



HAL
open science

Operating Conditions Effect over the Coupling Strength for Urban Aerial Ropeways

Daniel Estepa, Ronald Martinod, Carmen Paris, Fabio Pineda, Jorge Restrepo, Leonel Castañeda, Gustavo A Mejía

► **To cite this version:**

Daniel Estepa, Ronald Martinod, Carmen Paris, Fabio Pineda, Jorge Restrepo, et al.. Operating Conditions Effect over the Coupling Strength for Urban Aerial Ropeways. *Transport Problems = Problemy Transportu*, 2014, 9 (3), pp.5-14. hal-02182168

HAL Id: hal-02182168

<https://hal.science/hal-02182168>

Submitted on 12 Jul 2019

HAL is a multi-disciplinary open access archive for the deposit and dissemination of scientific research documents, whether they are published or not. The documents may come from teaching and research institutions in France or abroad, or from public or private research centers.

L'archive ouverte pluridisciplinaire **HAL**, est destinée au dépôt et à la diffusion de documents scientifiques de niveau recherche, publiés ou non, émanant des établissements d'enseignement et de recherche français ou étrangers, des laboratoires publics ou privés.

aerial ropeways; cable car; funicular; safety transport; strain gage

**Daniel ESTEPA, Ronald M. MARTINOD, Carmen E. PARIS, Fabio A. PINEDA
Jorge L. RESTREPO, Leonel F. CASTAÑEDA***

Universidad EAFIT

Cr. 49 N° 7 Sur – 50, Medellín, Colombia

Gustavo A. MEJÍA

Empresa de Transporte Masivo del Valle de Aburrá Limitada

Cll. 44 46-001, Bello, Colombia

**Corresponding author.* E-mail: <[rmartino](mailto:rmartino@eafit.edu.co)><[fpineda](mailto:fpineda@eafit.edu.co)><[jrestrep](mailto:jrestrep@eafit.edu.co)><[lcasta](mailto:lcasta@eafit.edu.co)>@eafit.edu.co

OPERATING CONDITIONS EFFECT OVER THE COUPLING STRENGTH FOR URBAN AERIAL ROPEWAYS

Summary. The present work is aimed to assess the operating conditions effect for urban aerial ropeways with a commercial usage, based on measurements obtained from an arrangement of sensors that record the coupling assembly behavior between the detachable gondola pod and the track rope. The work pays particular attention to the effect caused by external conditions due to the wind loads joined up with other parasite external effects, through the measurement of the engage strains. The cableway gondola continuous cycle has mono-cable of simple ring type.

WARUNKI EKSPLOATACJI MAJĄCE WPŁYW NA WYTRZYMAŁOŚĆ MIEJSKICH KOLEI LINOWYCH

Streszczenie. Niniejsza praca ma na celu ocenę efektywnych warunków pracy dla miejskich napowietrznych kolei linowych z praktyką przemysłową, na podstawie pomiarów uzyskanych z układem czujników, które rejestrują zachowanie gondoli w trakcie procesu wyprężania gondoli z liny. Praca zwraca szczególną uwagę na wpływ warunków zewnętrznych spowodowanych przez obciążenia wiatrem z dołączeniem innych obciążeń zewnętrznych, poprzez pomiar naprężeń w trakcie wprężania. Kolej gondolowa jednolinowa ma pojedynczą linię prostego typu pierścieniowego.

1. INTRODUCTION

The transport systems by aerial cable cars have been used extensively as transport systems for the people in tourist areas. However, in recent years, these transport systems have been increasingly used in densely populated urban areas [7]. The transport systems with gondola infrastructure and equipment use standardized elements of production, which do not consider certain conditions of specific operations (the design does not discriminate between a mean of transport for tourist passengers and other urban transport with continuous operation), however, the transport systems by gondolas are sensitive to external conditions [3]: (i) the terms and conditions of operation – live loads, operation frequency; (ii) environmental conditions – wind loads, temperature, moisture, corrosion, etc.; and (iii) system availability.

The continuous operation cycle in detachable ropeways is characterized by the fact that the gondola fastening to the track rope is performed by means of a coupling assembly attached to the gondola, called carrying jaw, which allows the gondola to release in stations [2]. At each station, the gondola is released from the track rope, slowing down and going on a lane which leads to low speed through an area of passengers loading-offloading. Before the next departure, the gondola accelerates again until it reaches the travel speed, and then is attached to the track rope by the carrying jaw closure. The carrying jaw then secures the gondola pod at any point in the track rope, so that it allows the interval coupling between the gondolas [7].

There are developments that relate to monitoring devices in the coupling force through proximity sensors, which measures the flexible elastic base deformation extent in the control ramp clutch control on the station [11]. Other developments relate to devices of the carrying jaw coupling strength measure, which uses a measuring element type load cell provisioned in the ramp clutch control [12, 13]. In these installations, the load cells use is inconvenient because of their complicated installation. The developments defined in the state-of-the-art do not fulfill the objective of this work because the stations are usually instrumented, to inspect the coupling force, therefore it does not allow gondola connection behaviour registration in the trip bays in inter-stations.

The present work is focused on evaluating the change in the coupling force between the gondola and the track rope, due to the operating condition fluctuation and environmental conditions. This work is drawn forth by the clamp-cable attaching force magnitude regardless of the fixation point.

2. DESCRIPTION OF THE OBJECT OF STUDY

This study has been applied to passenger vehicles belonging to a fleet of three independent operation lines of mass transportation by gondola-type aerial cable on a continuous cycle, mono-cable (simple ring) with a detachable release clamp device, which operates in the city of Medellín (Colombia). The transport system is similar in design and construction to the ones used for passengers transport in winter tourist areas (e.g. Daemyung-Korea, La Clusaz-France, Donovaly-Slovakia). The system has been manufactured by the company Pomagalski (France) and inaugurated on the year 2004, providing continuous service 360 day a year, 7 days a week, 20 hours a day. Tab. 1 presents the overall technical characteristics of the object of study.

The detachable carrying jaw device has the clutching function (during the journey inter-station) and release (during transit in station) of the vehicle to the track rope, providing the tightening force required to cancel the relative movements between the vehicle and the track rope, particularly on track bays with extreme slopes. The set of the carrying jaw is composed of 52 elements; Fig. 1 shows the main elements, defined as the set of basic fundamental structural elements that compose it.

The work focuses on the study of a carrying jaw's component loads condition record, called fixed jaw; this is the main element for the assembly of the carrying jaw. The fixed jaw joint the moving jaw allows the gondola coupling to the track rope, in addition, the fixed jaw articulates the principal shaft, the crosstie, spring's tags and movement wheels [4]. The fixed jaw is composed by the material 36NiCrMo16, with hardness HB350-390, and has a tension resistance of 850 MPa.

The journey of the gondola pod in inter-station is the general scenario during the system's commercial exploitation to assess the operating conditions effect; this scenario defines the load conditions made to the fixed jaw, in which the gondola pod must be fully engaged to the track rope, in addition, the full weight of the gondola pod is transmitted by the carrying jaw to the track rope.

Table 1

General features of the transport ropeway system

General features	Inter-station values		
	A-B	B-C	C-D
Travel stations (start-end)			
Inter-station length [m]	1001	1075	624
Height's difference [m]	102	40	167
Maximum slope [%]	82	88	44
Quant. towers [ud.]	8	15	8
Dist. between gondola pods [m]	60	60	60
Commercial speed [m/s]	5	5	5

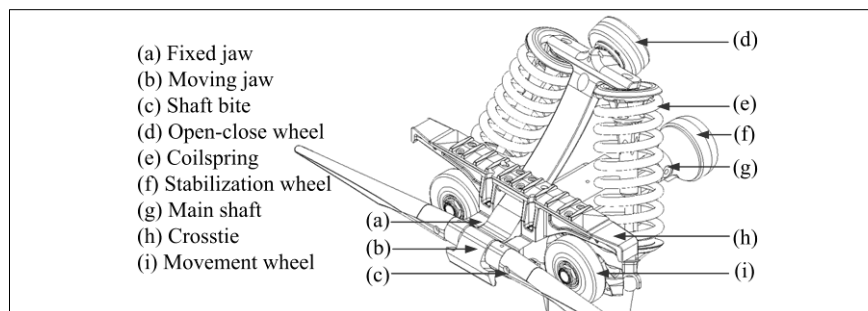


Fig. 1. Detachable carrying jaw main elements
Rys. 1. Główna część nośna szczęki ruchomej

3. DETERMINING THE INSPECTION POINT IN THE COUPLING ASSEMBLY

The determination of the inspection point in the carrying jaw is performed by means of a stress-strain distribution analysis in the fixed jaw generated in the load state. The stress-strain distribution analysis in this state was performed using a model in Finite Element Analysis (FEA). FEA is used to simulate the particular characteristics of the fixed jaw and it is considered a true virtual prototype. Virtual techniques allow the model to generate information of the behavior in the load state. The interaction of the components and details are comparable only with physical prototypes [5]. For the model construction in FEA, it is necessary to pose the static-elastic problem.

3.1. Static linear elasticity model approach

The continuous problems, including the mechanical structural problems and solids, can be solved based on the Principle of Minimum Potential Energy (PMPE). The PMPE establishes that the displacement $\{u\}$ that complies with the differential equations of equilibrium, as well as the boundary conditions on the surface, gives a minimum for the total potential energy in comparison with any other field of displacements that satisfy the same boundary conditions. Using the PMPE and considering an isotropic material in the elastic range –the material follows a linear function and a small $\{u\}$ response– can be determined $\{u\}$ and strains $\{\epsilon\}$ in the element.

3.2. FEA model development

The process for the analysis begins with the geometric modeling with a three-dimensional model generated by a CAD tool. The FEA model has been constructed from the following assumptions: (i) the components of the non-linear geometry are negligible in the system; (ii) the strains are made in the elastic material region; and (iii) the stress flows, that are located in areas outside the surface of interest, are not considered.

It is considered that the mass magnitude of the fixed jaw, m_t , is negligible in relation to the loads that flow while the releasing of the detachable carrying jaw. Consequently, for the load state, it is possible to state the system of balance equations as $\sum_{k=1}^N \{P\} = m_t \cdot \vec{a}_t = \vec{0}$, and $\sum \{M\} = \{I_t\} \cdot \vec{\rho}_t = \vec{0}$, where \vec{a}_t and $\vec{\rho}_t$ where \vec{a}_t and $\vec{\rho}_t$ denotes the linear acceleration and rotation respectively.

That is how the analysis is developed to find the forces closing equations system, which can be obtained by using any of the classical methods defined in the bodies mechanics (e.g. free body diagram), calculating the loads $\{P\}$ and moments $\{M\}$ in the load state, thereby defining the FEA model conditions. Fig. 6 and Tab. 3 (see Appendix A) details the FEA model frontier conditions. Tetrahedral elements were used to build a linear net with 126,719 elements, with a uniform size of 2.5mm.

3.3. Measuring point selection for the coupling strength inspection

A set of criteria to select the measuring point in the moving jaw has been established: (i) the measurement point must be feasible to the instrumentation; (ii) the measurement point must be such that the instrumentation does not interfere with the system's operation; and (iii) the measurement point must be located in a region with a surface range with enough sensitivity, for which a settlement of strain gages can properly record the strains $\{\varepsilon\}$.

Based on the FEA model results (see Fig. 7, Appendix B) the measurement point P is selected to the strain gauges fixing, the spatial position of measuring point P is shown in Fig. 2.a.

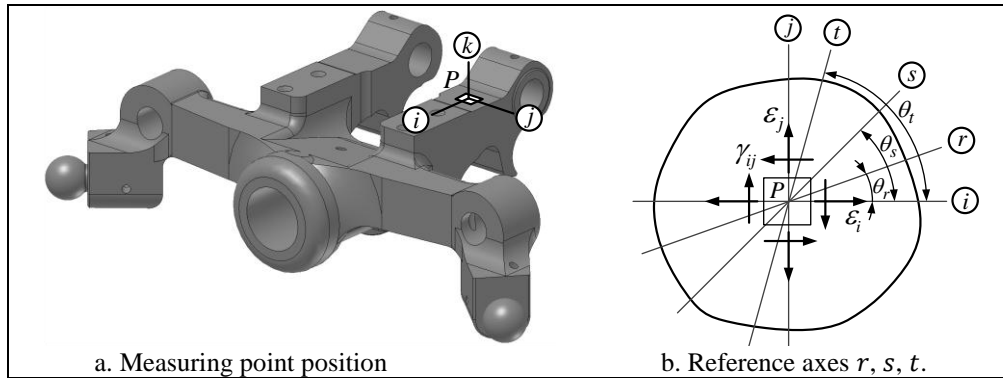


Fig. 2. Measuring point P in the fixed jaw

Rys. 2. Pomiar w punkcie P szczęki nieruchomej

4. DETERMINING THE INSPECTION POINT IN THE COUPLING ASSEMBLY

At the point P , it is appropriate to install an experimental arrangement to estimate the strains $\{\varepsilon_r, \varepsilon_s, \varepsilon_t\}$ in three reference axes r, s, t (see Fig. 2.b). This is done by using an arrangement of strain gages (resistive sensors sensitive to the variation of strains) attached to the surface of the point P . The recorded strains $\{\varepsilon_r, \varepsilon_s, \varepsilon_t\}$ are transmitted wirelessly to a data acquisition system, to process the information in real time.

4.1. Strains processing

Based on the recorded strains $\{\varepsilon_r, \varepsilon_s, \varepsilon_t\}$, it is possible to calculate the normal strains $\{\varepsilon_i, \varepsilon_j\}$, and shear strain $\{\gamma_{ij}\}$ in two axes (i and j), by means of one of the transformation methods for linear equation systems established in fields of geometric modeling, i.e. linear algebra, among others [9]. That is, the solution to the coordinate's axis transformation approach that allows calculating the

corresponding magnitudes of the variables to the strain states $\{\varepsilon_i, \varepsilon_j, \gamma_{ij}\}$ in the axes i and j , using the following expressions

$$\begin{aligned}\varepsilon_r &= f(\varepsilon_i, \varepsilon_j, \gamma_{ij}, \theta_r), \\ \varepsilon_s &= f(\varepsilon_i, \varepsilon_j, \gamma_{ij}, \theta_s), \\ \varepsilon_t &= f(\varepsilon_i, \varepsilon_j, \gamma_{ij}, \theta_t).\end{aligned}\quad (1)$$

The strains measurement is obtained on the point P surface, therefore, it is a plane strain case, Figure 2.b shows the status of the strains in the point P .

4.2. Experimental test validation

The validation of the experimental test is performed by means of checking between: (i) the test results in controlled operating conditions; and (ii) the calculation in FEA. The controlled test was made in quasi-static conditions and it has been performed in the workshop, i.e. the test has been isolated to external conditions and has the following features [10]: (i) without the wind loads effect; (ii) without operating frequency, due to a null gondola pod speed; (iii) with a constant temperature and moisture; and (iv) in the gondola pod, an equivalent of 700kg mass live load is applied. The calculations in FEA are obtained from a linear static model that emulates the existing conditions in the controlled test.

In the controlled test, the strain stationary data $\{\varepsilon_i, \varepsilon_j\}_{ctl}$ in the point P is processed. The FEA strains $\{\varepsilon_i, \varepsilon_j\}_{FEA}$ are computed in a point located analogue to the controlled test. Fig. 3 shows the Kaplan-Meier cumulative distribution to get a frequency density distribution (PDF) of the controlled quasi-static test and the strain mean $\{\bar{\varepsilon}_i, \bar{\varepsilon}_j\}_{ctl}$; it also presents the values obtained in FEA $\{\varepsilon_i, \varepsilon_j\}_{FEA}$. Then, from the $\{\bar{\varepsilon}_i, \bar{\varepsilon}_j\}_{ctl}$ and $\{\varepsilon_i, \varepsilon_j\}_{FEA}$ data, the measurement error, $e = \{e_i, e_j\}^T$, is calculated as follows

$$e = \begin{Bmatrix} e_i \\ e_j \end{Bmatrix} = \begin{Bmatrix} \frac{\varepsilon_{i(FEA)} - \bar{\varepsilon}_{i(ctl)}}{\varepsilon_{i(FEA)}} \\ \frac{\varepsilon_{j(FEA)} - \bar{\varepsilon}_{j(ctl)}}{\varepsilon_{j(FEA)}} \end{Bmatrix} \cdot 100 = \begin{Bmatrix} 0.45 \\ 1.32 \end{Bmatrix} [\%]. \quad (2)$$

A goodness of fit test was applied to the discrete variables of the controlled test, $\{\bar{\varepsilon}_i, \bar{\varepsilon}_j\}_{ctl}$, to determine the random degree in which it is constructed [14]. The probabilities adjustment establish that $\{\bar{\varepsilon}_i, \bar{\varepsilon}_j\}_{ctl}$ come from a set of adjusted distributions to the Gaussian probability (see Fig. 3), transforming the discrete variables to a continuous-theoretical variables [8], with the density function of a normal distribution variables, average values $\bar{\varepsilon}_{i,j}$ and variance values s^2 . The normal distribution fitting is considered valid given that the error values e represent an association measurement of the statistical model with the obtained data [6], which has an acceptable level for the scope of this work. Then, the results shows that there is an acceptable standard error relative to the fitting parameters (see Tab. 2), between experimental measurements and the model results from FEA.

Table 2

Normal fitting distribution parameters results

Parameter	$\{\varepsilon_i\}_{ctl}$	$\{\varepsilon_j\}_{ctl}$
Log likelihood	4.543E3	4.853E3
Mean [$\mu m / \mu m$]	0.524	0.135
Variance, s^2 [$\mu m / \mu m$]	2.059E-6	1.383E-6
Estimate [$\mu m / \mu m$]	$\bar{\varepsilon}$	0.524
	$\sqrt{s^2}$	1.435E-3
Std. Error	$\bar{\varepsilon}$	4.821E-5
	$\sqrt{s^2}$	3.412E-5

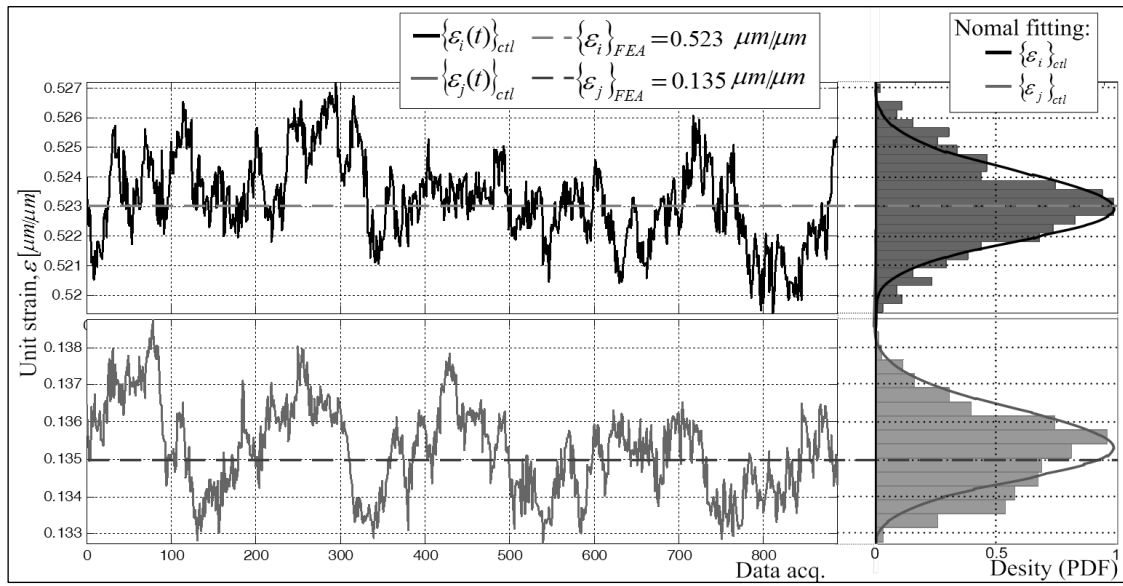
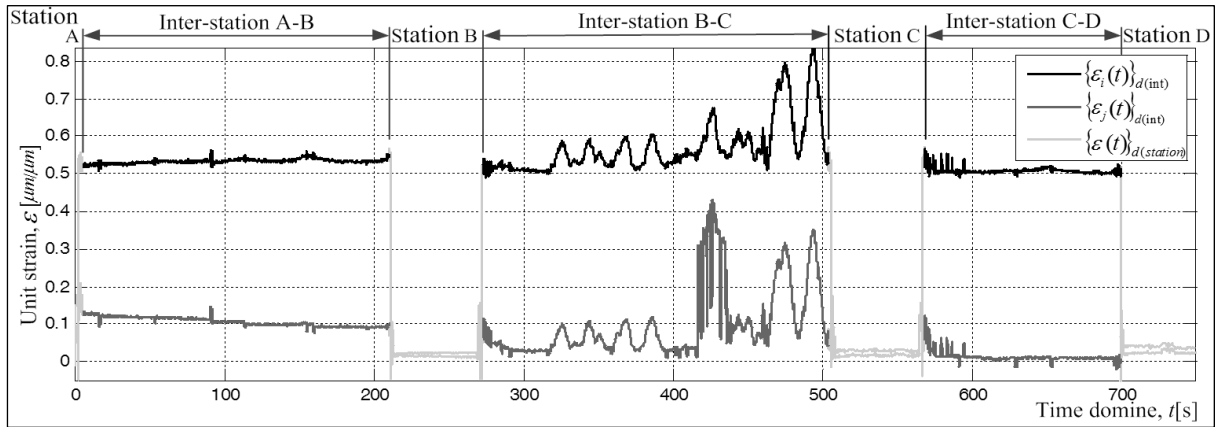


Fig. 3. Controlled test (quasi-static conditions)

Rys. 3. Badanie kontrolne (warunki quasi-statyczne)

5. ANALYSIS OF THE RESULTS

The gondola pod was subjected to a journey in commercial conditions in the entire circuit, (called dynamic conditions), getting the strains in the time domain $\{\varepsilon_i(t), \varepsilon_j(t)\}_d$. Then, the set of data is proceeded to extract the data segments in inter-stations, $\{\varepsilon_i(t), \varepsilon_j(t)\}_{d(int)}$ (see Fig. 4). The data segments $\{\varepsilon_i(t), \varepsilon_j(t)\}_{d(int)}$ record the wind loads effects joined up with other parasite external effects such as: (i) speed variation; (ii) disturbance caused by the entry and exit in the stations by the other gondolas pod; (iii) passengers movement inside the gondola pod; and (iv) disturbance caused by the gondolas transit on the towers. The Kaplan-Meier cumulative distribution of a set of strains $\{\varepsilon_i(t), \varepsilon_j(t)\}_{d(int)}$ is built to analyze the behavior of the sampled signals, which represent the description of the record in statistical terms (see Fig. 5); besides, it is shown the overlap of the signals $\{\varepsilon_i, \varepsilon_j\}$ by means of two histograms: (i) the gondola in controlled test $\{\varepsilon_i, \varepsilon_j\}_{ctl}$, described in the previous section; and (ii) the gondola in commercial conditions $\{\varepsilon_i(t), \varepsilon_j(t)\}_{d(int)}$. Due to the frequency histogram is characteristic of a normal distribution, it is estimated the average $\{\bar{\varepsilon}\} = \{[\bar{\varepsilon}_i, \bar{\varepsilon}_j]_{ctl}, [\bar{\varepsilon}_i, \bar{\varepsilon}_j]_{d(int)}\}$, as a measure of central tendency. In addition, it is possible to calculate the standard deviation $\{\sqrt{s^2}\} = \{[s_i, s_j]_{ctl}, [s_i, s_j]_{d(int)}\}$, as the dispersion of the measured signals caused by the effect of the wind loads and other external conditions.


 Fig. 4. Unit strain states $\{\varepsilon_i(t), \varepsilon_j(t)\}_{d(int)}$

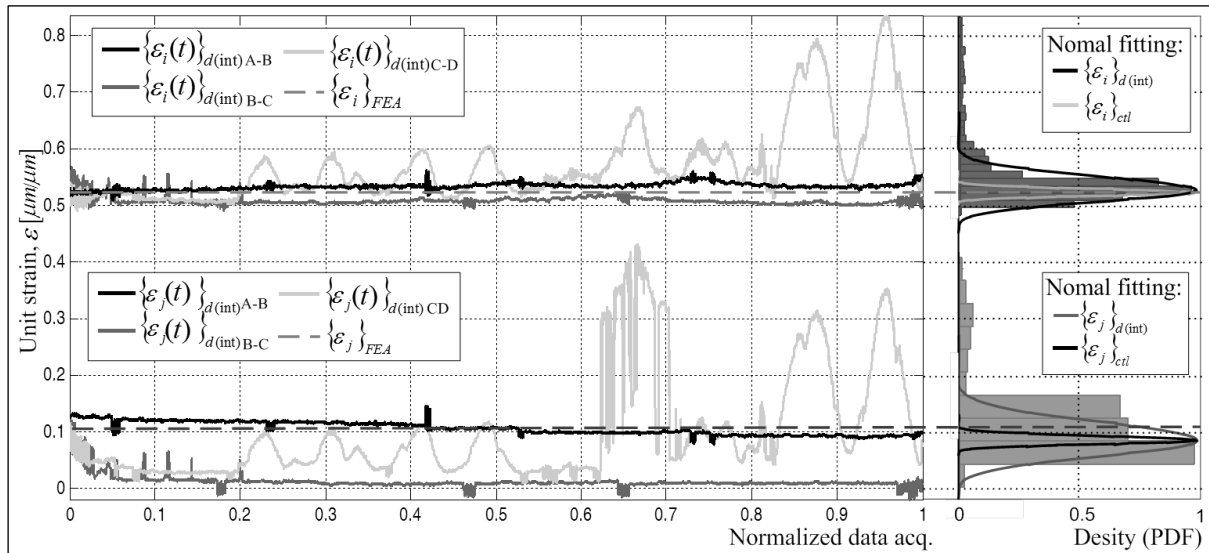
 Rys. 4. Jednostkowy stan naprężenia $\{\varepsilon_i(t), \varepsilon_j(t)\}_{d(int)}$


Fig. 5. Statistical description in inter-station journey

Rys. 5. Opis statystyczny w drodze między stacjami

The central tendency measures $\bar{\varepsilon}$ in both histograms to give approximate values $\bar{\varepsilon}_{i,ctl} \cong \bar{\varepsilon}_{i,d(int)}$ and $\bar{\varepsilon}_{j,ctl} \cong \bar{\varepsilon}_{j,d(int)}$ with an error, $e < 2.56\%$. This is because the records represent the detachable carrying jaw working with the live load carried by the gondola pod. However, the dispersion measures, quantified by the value of the standard deviation $s_{i,j} = [s_i, s_j]_{d(int)}$, have a different set of values $s_{i,ctl} \neq s_{i,d(int)}$ and $s_{j,ctl} \neq s_{j,d(int)}$; this is because the $[s_i, s_j]_{d(int)}$ value is directly proportional to the effect caused by external conditions. The Chebyshev theory provides a conservative estimation of the probability that a random variable takes within k standard deviations from its average to any k real number. The probability of the random variables $\varepsilon_{i,j} = \{\varepsilon_i, \varepsilon_j\}_{d(int)}$ taking value within k standard deviations $s_{i,j}$ from the mean, is at least $1 - 1/k^2$ [14], i.e.

$$P(\bar{\varepsilon}_{i,j} - k s_{i,j} < \varepsilon_{i,j} < \bar{\varepsilon}_{i,j} + k s_{i,j}) \geq 1 - \frac{1}{k^2}. \quad (3)$$

Therefore, around 99.7% of all the values from a normal distributed sample are within $\pm 3s_{i,j}$ from the mean $\bar{\varepsilon}_{i,j}$ [8], commonly known as the three-sigma rule, $\bar{\varepsilon}_{i,j} \pm 3s_{i,j}$. With $\varepsilon_{i,j(\max)} = \bar{\varepsilon}_{i,j} \pm 3s_{i,j}$ it is possible to infer, with a 99.7% certainty, that in the fixed jaw:

- (i) the maximum external excitation in direction i is $\varepsilon_{i(\max)} = 0.583 \mu\text{m}/\mu\text{m}$; and
- (ii) the maximum external excitation in direction j is $\varepsilon_{j(\max)} = 0.161 \mu\text{m}/\mu\text{m}$.

6. CONCLUSIONS AND FUTURE WORK

The standard deviation $\{s_i, s_j\}_{d(int)}$, as a statistical index applied to the strains $\{\varepsilon_i(t), \varepsilon_j(t)\}_{d(int)}$, is a sensitive index to record the effect caused by external shocks, by the effect of the wind loads and other parasite external effects such as: (i) speed variation; (ii) disturbance caused by the entry and exit in the stations by the other gondolas pod; (iii) passengers movement inside the gondola pod; and (iv) disturbance caused by the gondolas transit on the towers.

The proposed methodology can be used in operational conditions in each gondola pod. By defining a two standard deviations criterion (three-sigma rule), it is possible to classify the effect caused by external shocks: (i) in the case that the value of $\varepsilon_{i,j} > (\bar{\varepsilon}_{i,j} + 3s_{i,j})$, there is a relevant effect of disturbances due to the extreme conditions; or (ii) in the event that the histograms are similar $\varepsilon_{i,j} \leq (\bar{\varepsilon}_{i,j} + 3s_{i,j})$, it means that the effect of disturbances due to the extreme conditions, is not significant.

The proposed methodology gives the possibility of automating the process of ongoing inspection of the external excitation, for assessing the journey safety of a passenger cable car of urban transportation on aerial ropeways.

The proposed methodology is useful whereas the data logging allows getting information in commercial operation, avoiding measurements that require downtime for the system inspection.

The recorded signals allow the statistics analysis that can be used for maintenance planning; this means that the proposed procedure represents the technological basis for the development of the condition-based maintenance.

There is a clear feasibility to implement the proposed procedure for the entire fleet of aerial cable cars of urban aerial ropeway systems, because: (i) the sensors and data acquisition systems are widely studied for technical elements that do not represent a challenge to the current industrial sector; (ii) the costs of implementation are low in relation to the amount of information that the process may obtain from the system.

This paper opens to different research fields due to elements that can be considered for future publications: (i) to study the short pulses –with high frequency components– in $\varepsilon_{i,j}$ signal; (ii) to study the cable load and strain relative to the excitation frequencies effect; (iii) to study the relationship between the $\varepsilon_{i,j}$ variation and the aerial cable car faults to identify the technical state in commercial conditions.

References

1. Bathe, K.J. *Finite Element Procedures*. New Jersey, USA: Prentice Hall. 1996.
2. Bryja, D. & Knawa, M. Computational model of an inclined aerial ropeway and numerical method for analyzing nonlinear cable-car interaction. *Computers and Structures*. 2011. Vol. 89. No. 21. P. 1895-1905.
3. Degasperis, F. Measurement of dynamic stresses on carriers with detachable grip at station entrance: LA.T.I.F. experiences and future prospects. In: *8th International Congress for Transportation by Rope (OITAF)*. 1999. P. 107-133.
4. Doppelmayr, A. *Conceptual inputs for optimizing the functional efficiency of circulating monocable ropeways: project engineering, design and operation in a safety management control loop based on incident analysis*. Austria: WIR Public. 1998.

5. Genta, G. *Vibration Dynamics and Control*. Torino, Italy: Springer Science Business. 2009.
6. Grant, E.L. *Statistical Quality Control*. USA: McGraw Hill. 1964.
7. Hoffmann, K. Recent developments in cable-drawn urban transport systems. *FME Transactions*. 2006. Vol. 34. No. 4. P. 205-212.
8. Levin, R.I. & Rubin, D.S. *Statistics for management*. USA: Pearson. 2004.
9. O'Neil, P.V. *Advanced Engineering Mathematics*. Australia: Thomson. 2003.
10. Petrova, R. & Karapetkov, St. & Dechkova, S. & Petrov, P. Mathematical Simulation of Cross-Wind Vibrations in a Mono-Cable Chair Ropeway. *Procedia Engineering*. 2011. Vol. 14. P. 2459-2467.
11. Pomagalski, S.A. *Device for monitoring the spring force exerted by spring actuated bar coupled cable clamps for chair lifts and cable cars*. United States Patent and Trademark Office. US4665755: 1985.
12. Pomagalski, S.A. *Chairlift or gondola-lift having a friction-based driving device for chairs or cars*. United States Patent and Trademark Office. US5188037: 1993.
13. Pomagalski, S.A. *Device for remote measurement of clamping force of cable car or chair lift support cable clamp*. Institut National de la Propriété Industrielle. France. FR2750764-A1: 1996.
14. Walpole, R. & Myers, R. & Myers, S. & Keying, Y. *Probability & statistics for engineers & scientists*. USA: McGraw-Hill. 2011.
15. Zienkiewicz, O.C. & Morgan, K. *Finite Elements & Approximation*. USA: Dover Publications. 2006.

Appendix A. Boundary conditions applied to FEA model.

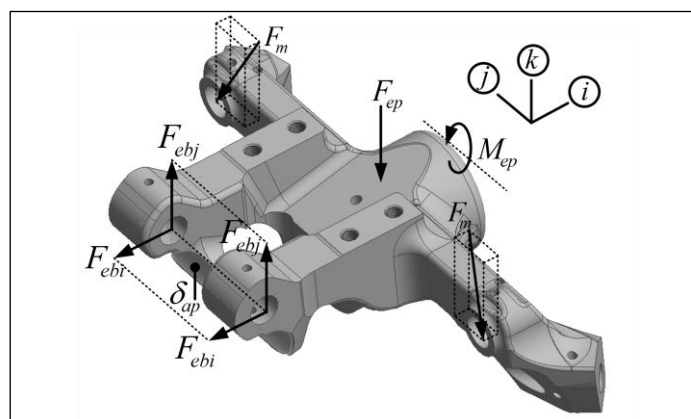


Fig. 6. Fixed jaw boundary conditions
 Rys. 6. Stałe warunki brzegowe szczęki

Table 3

Fixed jaw boundary conditions

Load	Value	Direction cosines [deg]		
		<i>i</i>	<i>j</i>	<i>k</i>
F_m [kN]	8.62	110	150	70
F_{ep} [kN]	14.5	90	0	90
F_{ebi} [kN]	76.9	0	90	90
F_{obj} [kN]	21.5	90	0	90
M_{ep} [kN m]	05.2	90	90	0
δ_{ap}	00.0	-	-	-

Appendix B. FEA planar strain flow.

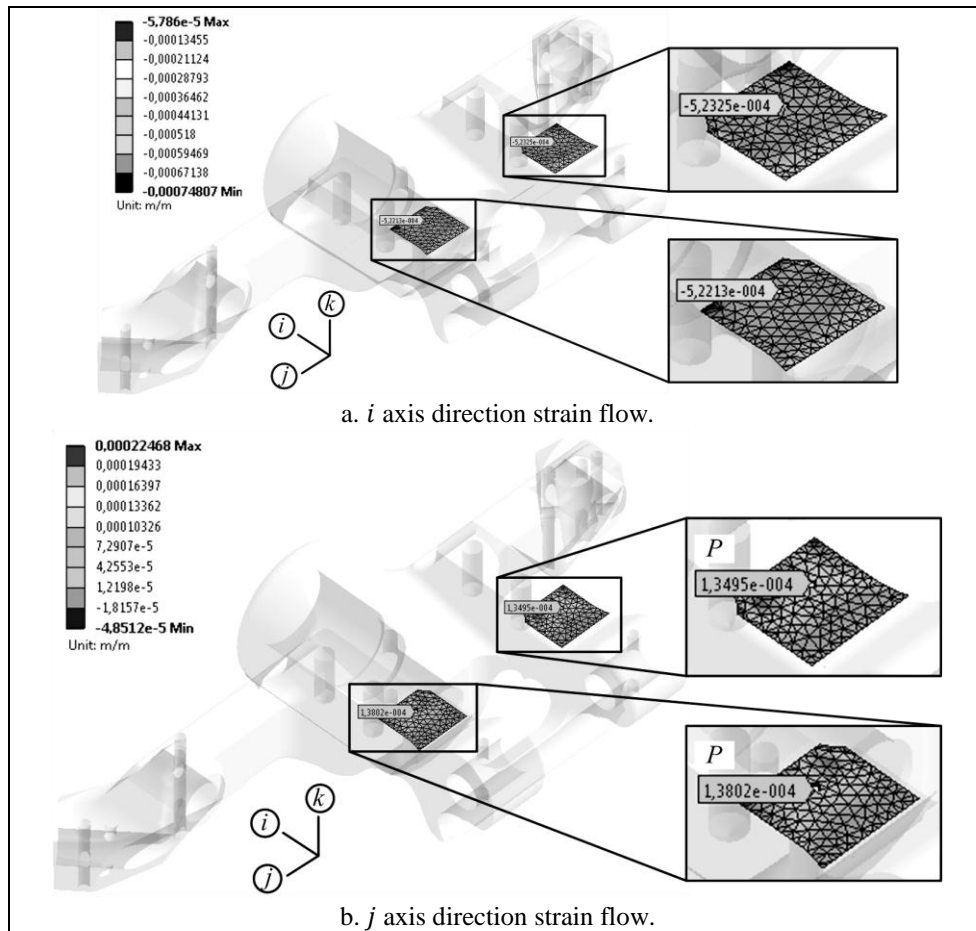


Fig. 7. Fixed jaw strain flow

Rys. 7. Rozkład naprężeń w szczęce stałej

Received 23.04.2013; accepted in revised form 25.08.2014